Available online at
www.ijacskros.com

Indian
Journal of Advances in
Chemical Science

Indian Journal of Advances in Chemical Science 3(2) (2015) 185-191

Effect of Temperature and Conduction Band Non-parabolicity on Electronic States in a Spherical Quantum Dot

A. Rejo Jeice[1], Sr. Gerardin Jayam[2], K.S. Joseph Wilson[3*]

[1]Department of Physics, Annai Velankannai College, Tholayavattam, Kanyakumari - 629 157, Tamil Nadu, India. [2]Department of Physics, Holy Cross College, Nagercoil - 629 002, Tamil Nadu, India. [3]Departmant of Physics, Arul Anandar College, Karumathur, Madurai - 625 514, Tamil Nadu, India.

Received 7th February 2015; Accepted 15th February 2015

ABSTRACT

The combined effect of temperature and conduction band non-parabolicity on the ground and low-lying excited states of an electron in a gallium arsenide spherical quantum dot (SQD) have been studied. The results are presented for the SQD with square well confinement corresponding to different values of x. Our result shows the: (i) The confined energies decreases as the dot size increases, (ii) it increases with increase within temperature, and (iii) further it decreases due to the application of conduction band non-parabolicity. All the calculations have been carried out with finite models, and the results are compared with existing literature.

Key words: *Spherical quantum dot, Temperature, Confined energies, Effective mass approximation.*

1. INTRODUCTION

An electron in a spherical quantum dot (SQD) has discrete energy levels as in an atom [1,2]. The study of these electronic levels is important to understand how such levels differ from the bulk [3,4]. Since the SQD exhibit discrete spectra, they are called artificial atoms [5,6]. Artificial atoms are important for most of their device application since they exhibit emission energies, number of excited states, coulomb interaction, etc., are determined by their confinement dimensions. Hence, quantum confinement is important in nanosystem [7]. In most of the previous investigation [8] they had restricted to calculate the lowest sub-band energies. The effects of the temperature dependence of the SQD have been studied by several authors [9-15].

Elabasy found that the binding energy of the donor electron, associated with the donor ion, decreases with enchaining the temperature [9,10]. John Peter and Navaneethakrishnan found that the application of temperature to the quantum well the binding energy decreases [11]. Rezaei and Shojaeian Kish studied the effect of temperature on impurity in a two-dimensional quantum dot have a great influence on the binding energy [12]. Khordad calculated the effect of temperature on the binding energy of excited states in a ridge quantum wire. He found that the impurity location play important roles in the binding energy of the ground state and two low-lying excited impurity states for a V-groove quantum wire [13]. Karki *et al*. studied the effect of temperature in cylindrical gallium arsenide (GaAs)-(Ga,Al) as quantum well wires at selected temperatures and found that the temperature is increased, the binding energy drops slightly [14]. Sivakami and Gayathri showed that the increment in temperature results decrease in correlation energy [15] and rise in temperature decrease in binding energy [16]. In the previous paper, one of the authors had studied the effect of hydrostatic pressure and polaronic mass on the correlation energies in an SQD [17].

In the present paper, a systematic study of variation of temperature and conduction band non-parabolicity as a function of dot size has been attempted in a finite confinement model. The purpose of the present work is two-fold. The first is to calculate the confined energy for 1s, 1p and 1d state with the variation of temperature. Second, we calculate the variation of conduction band non-parabolicity effect for the electronic states. The method followed is presented in the section 2 while the results and discussion are provided in section 3.

2. METHOD

2.1. Electron in an SQD

We consider a single electron in an SQD in the finite barrier model. In the absence of impurity, within the effective mass approximation, the Hamiltonian is given by

*Corresponding Author:
E-mail: wilsonpra@yahoo.co.in.
Phone: +91-9443774169

$$H_1 = -\frac{\hbar^2}{2m^*(T)}\nabla^2 + V_D(r,T) \quad (1)$$

Where m* is the effective mass of the electron at the conduction band minimum, which is $0.067m_0$ for GaAs [18], where m_0 is the free electron mass. In our numerical calculations we use atomic units in which $m_0=e^2=\hbar^2=1$. The confining potential $V_D(r)$ is given by [19,20]

$$V_D(r,T) = \begin{cases} 0 & r \le R \\ V_0 = Q_C \Delta E_g^\Gamma(x,T) & r \ge R \end{cases} \quad (2)$$

Where V_o is the barrier height, Q_c is the conduction band offset parameter which is taken to be 0.6 [1]. The band gap difference depends on the concentration of Al. In our case, $Ga_{1-x}Al_xAs$ is the barrier medium in which GaAs dot is embedded. The total energy difference [21] between the dot and barrier media, as a function of x, is given by

$$\Delta E_g^\Gamma(x) = 1.155x + 0.37x^2 \text{ eV} \quad (3)$$

In the present work we have chosen x=0.2 and 0.4 and the value of V_0 turns to be 147.48 and 312.72 meV, respectively. Two lowest lying three bound states are given by [4]

$$\psi_{1s}(\vec{r}) = \begin{cases} N_1 \frac{\sin(\alpha_1 r)}{\alpha_1 r} & r \le R \\ A_1 \frac{e^{-\beta_1 r}}{\beta_1 r} & r \ge R \end{cases} \quad (4)$$

$$\psi_{1p}(\vec{r}) = \begin{cases} N_2 \left(\frac{\sin(\alpha_1 r)}{(\alpha_2 r)^2} - \frac{\cos(\alpha_2 r)}{\alpha_2 r} \right) \cos\theta & r \le R \\ iA_2 \left(\frac{1}{\beta_2 r} + \frac{1}{(\beta_2 r)^2} \right) e^{-\beta_2 r} \cos\theta & r \ge R \end{cases} \quad (5)$$

$$\psi_{1d}(\vec{r}) = \begin{cases} N_3 \left(\left(\frac{3}{(\alpha_3 r)^3} - \frac{1}{\alpha_3 r} \right) \sin(\alpha_3 r) - \frac{3}{(\alpha_3 r)^2} \cos(\alpha_3 r) \right) (3\cos^2\theta - 1) & r \le R \\ A_3 \left(\frac{1}{\beta_3 r} + \frac{1}{(\beta_3 r)^2} + \frac{1}{(\beta_3 r)^3} \right) e^{-\beta_3 r} (\cos^2\theta - 1) & r \ge R \end{cases} \quad (6)$$

Where N_1, N_2, N_3, A_1, A_2 and A_3 are normalization constants and α_1 and β_1 are given by $\alpha_1 = \sqrt{2m^* E}$ and $\beta_1 = \sqrt{2m^*(V_o - E)}$

Matching the wave function and their derivatives at the boundary r=R, we get

$$A_1 = N_1 \sin(\alpha_1 R) e^{\beta_1 R} \quad (7)$$

$$A_2 = -iN_2 \left(\frac{\beta_2}{\alpha_2} \right)^2 \left(\frac{\sin(\alpha_2 R) - \alpha_2 R \cos(\alpha_2 R)}{\beta_2 R + 1} \right) e^{\beta_2 R}$$

$$A_3 = N_3 \left(\frac{\beta_2}{\alpha_2} \right)^2 \left(\frac{(3 - (\alpha_3 R)^2 \sin(\alpha_3 R) - 3\alpha_3 R \cos(\alpha_3 R)}{(\alpha_3 R)^2 + 3\beta_3 R + 3} \right) e^{\beta_3 R}$$

The energy Eigen values are determined by imposing the Ben Daniel and Duke boundary condition that the normal particle velocity is continuous across the interface [22]

$$-\frac{i\hbar}{m_1^*} \frac{\partial \psi}{\partial r}(r \le R)\Big|_{r=R} = -\frac{i\hbar}{m_2^*} \frac{\partial \psi}{\partial r}(r \ge R)\Big|_{r=R}$$

We obtain $\alpha_1 R + \beta_1 R \tan(\alpha_1 R) = 0$ s-states

$$\frac{\cot(\alpha_2 R)}{\alpha_2 R} - \frac{1}{(\alpha_2 R)^2} = \frac{1}{\beta_2 R} + \frac{1}{(\beta_2 R)^2} \quad \text{p-states}$$

$$(9\alpha_3 R - ((\alpha_3 R)^3) + (4(\alpha_3 R)^2 - 9)\tan(\alpha_3 R) == -\left[(3 - (\alpha_3 R)^2 \tan(\alpha_3 R) - 3(\alpha_3 R) \right] * \left[\frac{(\beta_3 R)^3 + 4(\beta_3 R)^2 + 9(\beta_3 R) + 9}{(\beta_3 R)^2 + 3(\beta_3 R) + 3} \right] \quad \text{d-states}$$

If $m_1^* = m_2^* = m^*$, solving these transcendental equations numerically, the confined energies E_1^n (n=1, 2, 3…; L=0, 1, 3) are obtained. For other excited states, similar equations may be obtained when L=3, 4,… The confined energy for the first three states for the barrier heights is given in Tables 1-6.

2.2. Effect of Conduction Band Non-parabolicity

The conduction band of GaAs is known to have non-parabolicity and a correction to the effective mass pertinent to the conduction band minimum are given [23] by

$$m_{np}^*(P) = 0.067 \left[1 + \frac{\Gamma_E}{0.067} \right] \quad (8)$$

Where $\Gamma_E = 0.0436 + 0.23E^2 - 0.147E^3$ in which E is the confined energy expressed in eV.

Table 1: Confined energies (meV) under temperature in the finite barrier model for E_{1s} state (x=0.2).

Dot radii (Å)	T=0 K	T=200 K	T=400 K	T=500 K
35	136.71 (142.74)	137.89 (143.77)	139.85 (145.35)	140.91 (146.07)
40	123.39 (130.69)	124.8 (132.34)	127.35 (135.15)	128.41 (140.91)
50	98.58 (104.53)	100.16 (106.44)	102.91 (109.84)	104.47 (111.77)
100	37.74 (38.66)	38.67 (39.68)	40.34 (41.50)	41.31 (42.59)
150	19.21 (19.44)	19.73 (20)	20.7 (21.00)	21.25 (21.59)
200	11.55 (11.64)	11.88 (11.98)	12.49 (12.60)	12.85 (12.96)
250	7.69 (7.73)	7.92 (7.95)	8.34 (8.38)	8.58 (8.64)
300	5.49 (5.50)	5.65 (5.66)	5.95 (5.99)	6.12 (6.15)

Numbers within brackets refer to the confined energies in the absence of band non-parabolicity effect

Table 2: Confined energies (meV) under temperature in the finite barrier model for E_{1s} state (x=0.4).

Radii (Å)	T=0 K	T=200 K	T=400 K	T=500 K
30	216.79 (256.07)	218.99 (260.00)	222.75 (266.77)	224.83 (270.58)
35	185.52 (216.74)	187.79 (220.80)	191.6 (227.98)	193.73 (232.07)
40	160.00 (183.47)	162.27 (187.31)	166.15 (194.15)	168.32 198.11)
50	121.37 (134.32)	123.53 (137.50)	127.30 (143.20)	129.44 146.52)
100	42.16 (43.43)	43.26 (44.65)	45.24 (46.86)	46.41 (48.19)
150	20.73 (21.02)	21.31 (21.62)	22.38 (22.76)	23.03 (23.43)
200	12.24 (12.34)	12.59 (12.70)	13.27 (13.38)	13.65 (13.80)
250	8.05 (8.10)	8.30 (8.35)	8.75 (8.81)	9.01 (9.08)
300	5.70 (5.72)	5.88 (5.91)	6.20 (6.23)	6.38 (6.42)

Numbers within brackets refer to the confined energies in the absence of band non-parabolicity effect

Table 3: Confined energies (meV) under temperature in the finite barrier model for E_{1p} state (x=0.2).

Dot radii (Å)	T=0 K	T=200 K	T=400 K	T=500 K
65	129.69 (140.75)	131.6 (143.01)	134.92 (146.67)	-
100	73.63 (77.73)	75.25 (79.70)	78.14 (83.22)	79.80 (85.31)
150	38.53 (39.57)	39.55 (40.68)	41.36 (42.70)	42.45 (43.88)
200	23.38 (23.75)	24.03 (24.44)	25.22 (25.71)	25.93 (26.45)
250	15.64 (15.8)	16.09 (16.27)	16.92 (17.12)	17.4 (17.63)
300	11.15 (11.25)	11.51 (11.58)	12.1 (12.20)	12.46 (12.57)

Numbers within brackets refer to the confined energies in the absence of band non-parabolicity effect. -: Un bound state

Table 4: Confined energies (meV) under temperature in the finite barrier model for E_{1p} state (x=0.4).

Radii (Å)	T=0 K	T=200 K	T=400 K	T=500 K
50	210.06 (261.17)	212.35 (266.50)	216.23 (275.83)	218.34 (281.14)
65	153.85 (179.56)	156.27 (183.96)	160.41 (191.93)	162.70 (196.60)
100	82.41 (88.35)	84.32 (90.80)	87.72 (95.26)	89.69 (97.92)
150	41.62 (42.90)	42.75 (44.16)	45.80 (46.47)	46.00 (47.84)
200	24.79 (25.22)	25.50 (25.97)	26.8 (27.36)	27.57 (28.19)
250	16.39 (16.56)	16.87 (17.08)	17.76 (18.00)	18.3 (18.55)
300	11.61 (11.70)	11.99 (12.07)	12.61 (12.72)	13.00 (13.12)

Numbers within brackets refer to the confined energies in the absence of band non-parabolicity effect

Table 5: Confined energies (meV) under temperature in the finite barrier model for E_{1d} state (x=0.2).

Radii (Å)	T=0 K	T=200 K	T=400 K	T=500 K
100	113.58 (124.58)	115.69 (127.49)	119.375 (132.65)	121.46 (135.65)
150	61.73 (64.71)	63.25 (66.49)	65.96 (69.73)	67.54 (71.66)
200	37.93 (38.98)	38.96 (40.10)	40.83 (42.16)	41.92 (43.38)
250	25.5 (25.95)	26.23 (26.71)	27.55 (28.13)	28.33 (28.96)
300	18.27 (18.50)	18.8 (19.05)	19.78 (20.07)	20.36 (20.68)

Numbers within brackets refer to the confined energies in the absence of band non-parabolicity effect

Table 6: Confined energies (meV) under temperature in the finite barrier model for E_{1d} state (x=0.4).

Radii (Å)	T=100 K	T=200 K	T=400 K	T=500 K
65	220.36 (287.79)	221.81 (292.00)	225.43 (303.03)	227.39 (309.25)
75	186.99 (233.13)	188.58 (236.98)	192.51 (247.29)	194.62 (253.30)
100	127.78 (145.65)	129.41 (148.30)	133.62 (155.50)	135.98 (159.75)
150	67.22 (71.13)	68.37 (72.52)	71.41 (76.28)	73.18 (78.52)
200	40.59 (41.85)	41.34 (42.69)	43.38 (44.97)	44.58 (46.33)
250	26.98 (27.51)	27.51 (28.08)	28.93 (29.60)	29.77 (30.51)
300	19.19 (19.45)	19.57 (19.85)	20.61 (20.93)	21.23 (21.59)

Number within brackets refer to the confined energies in the absence of band non-parabolicity effect

2.3. Effect of Temperature

Due the application of temperature, the effective mass and the barrier height are modified. The total band gap difference between the GaAs and $Ga_{1-x}Al_xAs$ barrier medium under the influence of heat is given by [9,24]

$$\Delta E_g^{\Gamma}(x,T)= \Delta E_g^{\Gamma}(x)+G(x)T \quad (9)$$

Where $G(x) = [-(1.15\times10^{-4})] \times eV/K$

The temperature dependent conduction effective masses of the quantum dot and barrier layer are obtained from the expression [25]

$$\frac{m_e}{m^*(T)} = 1+E\left\{\frac{2}{E_g^{\Gamma}(T)}+\left(E_g^{\Gamma}(T)+\Delta_0\right)^{-1}\right\} \quad (10)$$

Where E=7.51eV, is the energy related to the momentum matrix element. Δ_0=0.341 eV is the spin-orbit splitting, me is the free electron mass and Ep(T) is the temperature-dependent energy gap for the GaAs QD at the τ-point and is given by [26]

$$E_g^{\Gamma}(T) = 1.519-\frac{(5.405\times10^{-4})T^2}{(T+204)} \quad (11)$$

Corresponding conduction effective mass in the barrier layer is obtained from a linear interpolation between the GaAs and AlAs compounds' [15] i.e.,

$$m_b^*(T) = m_{w*}^*(T)+0.083x \quad (12)$$

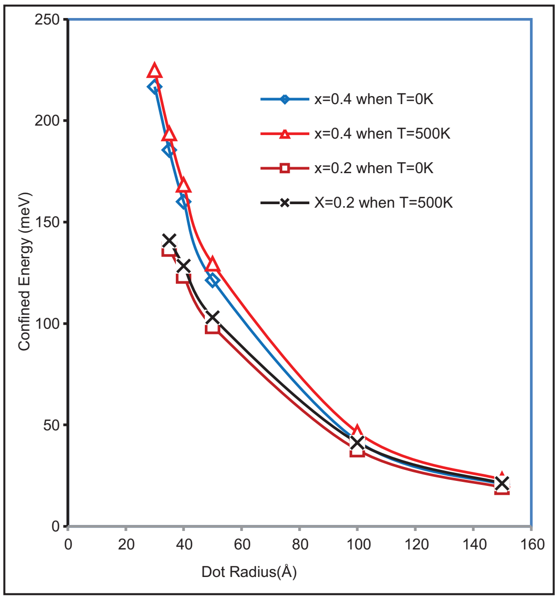

Figure 1: Variation of confined energy verses dot radius in the finite barrier model for E_{1s} state with band non-parabolicity effect.

Where x is the mole fraction of aluminum in the GaAlAs layer.

3. RESULTS AND DISCUSSION

The results obtained are shown in Tables 1-6 and Figures 1-5. We have computed the combined effect of temperature and conduction band non-parabolicity on electronic states on the SQD. Due the application of the temperature on the SQD, the effective mass and the barrier height of the dot radius are modified. We

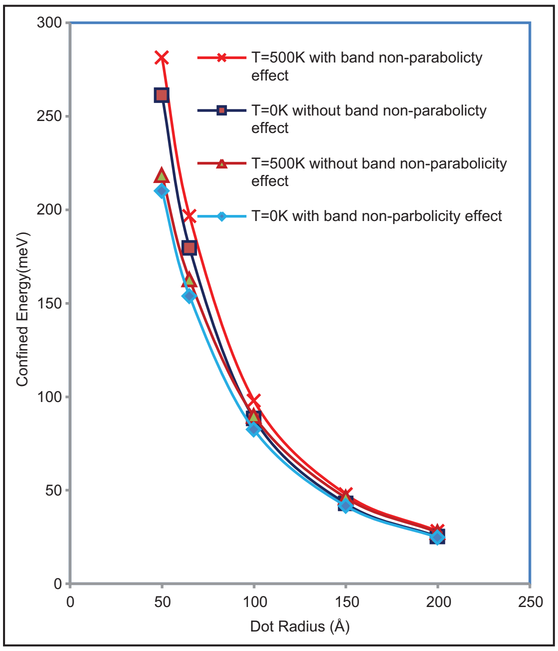

Figure 2: Variation of confined energy verses dot radius in the finite barrier model for E_{1p} state for x=0.4.

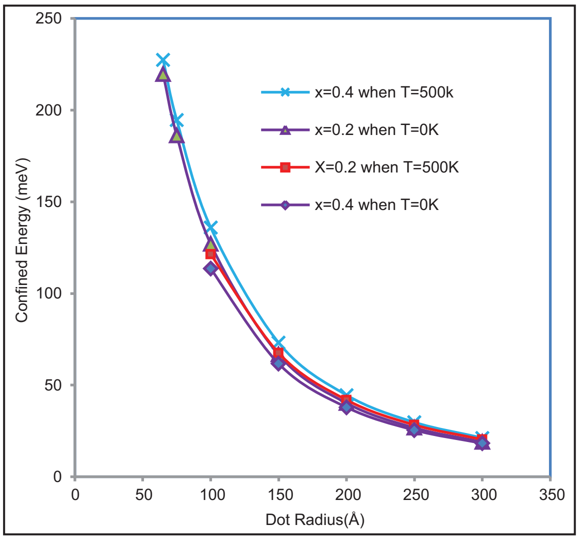

Figure 3: Variation of confined energy verses dot radius in the finite barrier model for E_{1d} state.

have noticed that due to the application temperature the effective mass and the barrier height slightly decreases. The variation of confined energies with dot radius for the barrier concentration x=0.2 and 0.4 for E_{1s}, E_{1p} and E_{1d} states are given in Tables 1-6.

From Tables 1-6, we find that the confined energy decreases as the dot radius increases which is well known in the literature [27,28]. For a given dot radius as the temperature increases the energy also increases which is a contract with the application of pressure in the SQD [29]. For the application of the conduction band non-parabolicity the energy decreases as well known in the literature [30]. We also notice that the

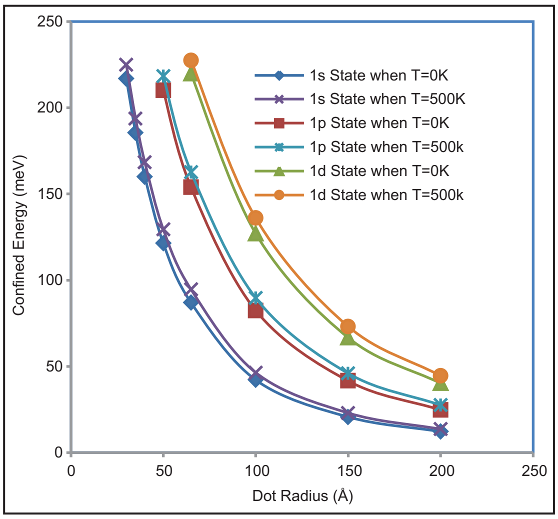

Figure 4: Variation of confined energy for different dot radius with conduction band non-parabolicity when x=0.4.

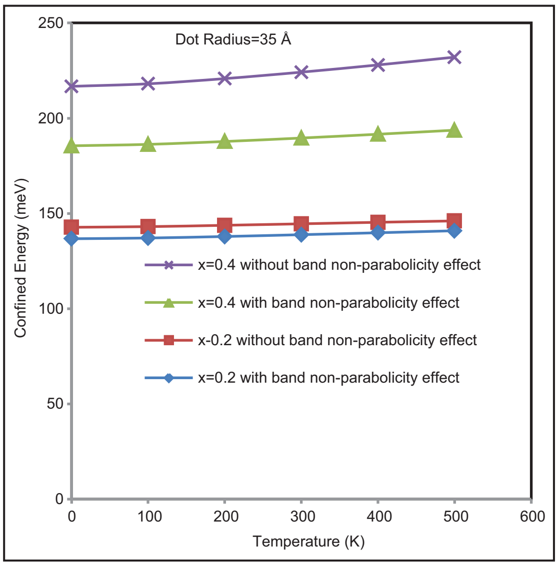

Figure 5: Variation of confined energy with temperature for the dot radius of 35 Å for E_{1s} state.

absence of the band non-parabolicity the confinement decreases when the temperature increases for all dot size. This behavior is due to variation of mass with the change in sub band energy.

From Tables 1-2, we find that the confined energy increases with an increase in aluminum concentration and temperature. The increase in confinement is 3% for x=0.2 and 4% for x=0.4, respectively. The effect of conduction band parabolicity also reduces the energy value 4% for lower dot radius when x=0.2 and 18-20% when x=0.4. For smaller dot sizes <3 Å we notice there is no confinement energy for 1s-state (when x=0.4) since there is no bound state. These results contrast for the quantum well case wherein there is a bound state for every well size [21].

From Tables 3 and 4, we find that the confinement is 2-4% for lower dot radius with increase in temperature. The effect of conduction band parabolicity reduces 20-28% for x=0.2 and x=0.4 respectively. From Tables 5 and 6, we find that the confinement is 7-8% for lower dot radius with increase in temperature. The effect of conduction band parabolicity reduces 30-38% for x=0.2 and x=0.4, respectively. Another observation from the tables that we have not considered the value of x beyond x=0.4.Since the indirect band gap nature in $Ga_{1-x}Al_xAs$ [31].

Figure 1 represents the variation of confined energy for different dot radius for E_{1s} state with band non-parabolicity effect for temperature T=0K to T=500K. We notice there is an increase in confinement with temperature. Figure 2 represent the variation of confined energy for different dot radius in the finite barrier model for E_{1p} state for x=0.4. Here we notice the percentage of variation is more than that of the ground state. Figure 3 represents the variation of confined energy for different dot radius in the finite barrier model for E_{1d} state. For higher aluminum concentration, the confinement is more than lower concentration. Figure 4 represent the variation of confined energy for different dot radius with conduction band non-parabolicity when x=0.4 for the three low-lying states. It clearly shows that the ground state energy is shifted towards the lower dot radius. When the dot radius is very larger, the confined energies show three-dimensional behavior.

Figure 5 we display the variation of confined energy with temperature for the dot radius of 35 Å for the barrier concentration 0.2 and 0.4, respectively, in the ground state. It has been seen that the temperature increases the confined energy increases linearly. The important conclusion that emerges from the result of Tables 1-6 and Figures 1-5 is that the temperature and conduction band non-parabolicity effect are important for smaller dots and should be considered in the studies of low-dimensional semiconductor systems.

4. CONCLUSION

A systematic investigation of a single-electron quantum dot has been presented. We investigated the effects of temperature and conduction band non-parabolicity on the confined energies in GaAs/$Ga_{1-x}Al_xAs$ SQD. We found that the confinement is important in nanosystems of smaller dot radius, and it approaches to zero as the dot size approaches infinity. The effect of temperature reduces the confinement to 2-8%, and conduction band non-parabolicity reduces 4-38% in the above electronic states. We can tune the band gap of the SQD using concentration of the barrier material. The tunability of the band gap of the SQD plays a significant role in luminescent and photovoltaic devices.

5. ACKNOWLEDGMENTS

The authors would like to thank Prof. K. Navaneethakrishnan, School of Physics, Madurai Kamaraj University, Madurai, India for his valuable and useful suggestions.

6. REFERENCES

1. R. S. D. Bella, K. Navaneethakrishnan, (2004) Donor binding energies and spin-orbit coupling in a spherical quantum dot, ***Solid State Communications*, 130(11):** 773-776.
2. A. John Peter, (2005) The effect of hydrostatic pressure on binding energy of impurity states in spherical quantum dots, ***Physica E: Low-dimensional Systems and Nanostructures,* 28(3):** 225-229.
3. A. Rejo Jeice, K. Navaneethakrishnan, (2009) Correlation energy in a triplet state of a two electron quantum dot, ***Brazalian Journal of Physics,* 39(3):** 526-530.
4. M. A. Kastner, (2000) The single electron transistor and artificial atoms, ***Annalen der Physik,* 9(11-12):** 885-894.
5. C. Yannouleas, U. Landman, (2002) Strongly correlated wavefunctions for artificial atoms and molecules, ***Journal of Physics: Condensed Matter,* 14:** L591-L598.
6. S. Bednarek, B. Szafaran, J. Adamowski, (1990) Many-electron artificial atoms, ***Physical Review B,* 59:** 13036-13042.
7. G. Cantele, D. Ninno, G. Iadonisi, (2001) Shape effects on the one and two electron ground state in a ellipsoidal quantum dots, ***Physical Review B,* 64(1-8):** 125325.
8. A. Sivakami, K. Navaneethakrishnan, (2008) Correlation energy in a spherical quantum dot, ***Physica E*, 40:** 649-653.
9. A. M. Elabasy, (1992) Temperature dependence of shallow donor states in GaAs-$Al_xGa_{1-x}As$ compostional superlattice, ***Physica Scripta*, 46:** 473-475.
10. A. M. Elabasy, (1999) Effect of temperature on the binding energy of a confined impurity to a spherical semiconductor quantum dot, ***Physica Scripta*, 59:** 328-330.
11. A. John Peter, K. Navaneethakrishnan, (2003) Simultaneous effects of pressure and temperature on donors in a GaAlAs/GaAs quantum well, ***Superlattices and Microstructrues*, 43:** 63-70.
12. G. Rezaei, S. Shojaeian Kish, (2012) Effects of external electric and magnetic fields, hydrostatic pressure and temperature on the binding energy of a hydrogenic impurity confined in a two-dimensional quantum dot, ***Physica E,* 45:** 56-60.
13. R. Khordad, (2009) Effect of temperature on the binding energy of excited states in a ridge quantum wire, ***Physica E,* 41:** 543-546.
14. H. D. Karki, S. Elagoz, P. Baser, (2011) The high hydrostatic pressure effect on shallow donor

binding energies in GaAs–(Ga,Al) As cylindrical quantum well wires at selected temperatures, ***Physica B,*** **406:** 2116-2120.
15. A. Sivakami, V. Gayathri, (2013) Hydrostatic pressure and temperature dependence of dielectric mismatch effect on the impurity binding energy in a spherical quantum dot, ***Superlattices and Microstructructures*****, 58:** 218-227.
16. A. Sivakami, M. Mahendran, (2010) Hydro – static pressure and temperature dependence of correlation energy in a spherical quantum dot, ***Superlattices and Microstructructures*****, 47:** 530-537.
17. A. Sivakami, A. Rejo Jeice, K. Navaneethakrishnan, (2010) Effects of hydrostatic pressure and polaronic effects on the correlation energies in a spherical quantum dot, ***International Journal of Modern Physics B*****, 24:** 5561-5569.
18. O. Madelung (Ed.), (1996) ***Semiconductor Basic Data,*** 2nd Revised Edition. London: Springer-Verlag.
19. E. Kasapoglu, H. Sari, I. Sökmen, (2006) Shallow donors in the triple-graded quantum well under the hydrostatic pressure and external fields, ***Physica B,*** **373:** 280-283.
20. A. Rejo Jeice, K. S. Joseph Wison, (2013) Effect of temperature and pressure on correlation energy in a triplet state of a two electron spherical quantum dot, ***Journal of Nanostructures*****, 3:** 347-357.
21. V. V. Mitin, V. A. Kochelap, M. A. Stroscio, (1999***) Micro Electronics and Optoelectronics,*** Cambridge: Cambridge University Press.
22. Y. Li, O. Voskoboynikov, J. L. Liu, C. P. Lee, S. M. Sze, (2001) Spin dependent boundary conditions and spin splitting in cylindrical quantum dots, ***Nanotechnology,*** **1:** 562-565.
23. S. Chaudhuri, K. K. Bajaj, (1984) Effect of nonparabolicity on the energy levels of hydrogenic donors in GaAs-Ga1-xAlxAs quantum-well structures, ***Physical Review B,*** **29:** 1803-1806.
24. B. Welber, M. Cardona, C. K. Kim, S. Rodriquez, (1975) Dependence of the direct energy gap of GaAs on hydrostatic pressure, ***Physical Review B,*** **12:** 5729-5738.
25. E. Kasapoglu, (2008) The hydrostatic pressure and temperature effects on donor impurities in GaAS/Ga1-xAlxAs double quantum well under the external fields, ***Physics Letters A,*** **373:** 140-143.
26. D. E. Aspnes, (1976) GaAs lower conduction-band minima: Ordering and properties, ***Physical Review B,*** **14:** 5331-5342.
27. G. Jeyam, K. Navaneethakrishnan, (2003) Effects of electric field and hydrostatic pressure on donor binding energies in a spherical quantum dot, ***Solid State Communications,*** **126(12):** 681-685.
28. S. Rajashabala, K. Navaneethakrishnan, (2008) Effects of dielectric and position dependent effective mass on donor binding energies and on diamagnetic susceptibility in a quantum well, ***Superlattices and Microstructures,*** **43(3):** 247-261.
29. G. Rezaei, N. A. Doostimotlagh, B. Vaseghi, (2011) Simultaneous effects of hydrostatic pressure and conduction band non-parabolicity on binding energies and diamagentic susceptibility of a hydrogenic impurity in spherical quantum dots, ***Communication Theoretical Physics,*** **56:** 377-381.
30. A. Sivakami, M. Mahendran, (2010) Hydrostatic pressure and conduction band non-parabolicity effects on the impurity binding energy in a spherical quantum dot, ***Physica B*****, 405:** 1403-1407.
31. A. John Peter, S. Saravanakumar, (2008) Two interacting electrons in low-lying states in a spherical quantum dot, ***Physica E*****, 41:** 138-141.

***Bibliographical Sketch**

Dr. KS Joseph Wilson Ph.D in Physics in Madurai Kamaraj University in Madurai .Now he is working as Associate Professor and Vice Principal in Arul Anandar College,Karumathur,Madurai-625514,India.He had 25 years of teaching experience. He is a Life member of Indian Association of Physics Teachers, Life member of Magnetic Society of India, Life Member of Photonic Society of India and Life Member in Global Science and Technology Forum, Singapore.